

Robust high order discontinuous Galerkin schemes for two-dimensional gaseous detonations

Cheng Wang¹, Xiangxiong Zhang², Chi-Wang Shu³ and Jianguo Ning⁴

Abstract

One of the main challenges in computational simulations of gas detonation propagation is that negative density or negative pressure may emerge during the time evolution, which will cause blow-ups. Therefore, schemes with provable positivity-preserving of density and pressure are desired. First order and second order positivity-preserving schemes were well studied, e.g., [6, 10]. A simple solution for arbitrarily high order positivity-preserving schemes solving Euler equations was proposed recently in [22]. For high order discontinuous Galerkin (DG) method, even though the characteristicwise TVB limiter in [1, 2] can kill oscillations, it is not sufficient to maintain the positivity. In this paper, we first discuss an extension of the technique in [22, 23, 24] to design arbitrarily high order positivity-preserving DG schemes for reactive Euler equations. We then present a simpler and more robust implementation of the positivity-preserving limiter than the one in [22]. Numerical tests, including very demanding examples in gaseous detonations, indicate that the third order DG scheme with the new positivity-preserving limiter produces satisfying results even without the TVB limiter.

AMS subject classification: 65M60, 76N15

Keywords: discontinuous Galerkin method; positivity preserving; high order accuracy; gaseous detonations

¹State Key Laboratory of Explosion Science and Technology, Beijing Institute of Technology, Beijing, 100081, P.R. China. E-mail: wangcheng@bit.edu.cn. Research supported by NSFC grants 11032002 and 10972040, National Basic Research Program (Grant No. 2011CB706904), and the Foundation of State Key Laboratory of Explosion Science and Technology (Grant No. ZDKT11-01).

²Department of Mathematics, Brown University, Providence, RI 02912. E-mail: zhangxx@dam.brown.edu. Research supported by AFOSR grant FA9550-09-1-0126.

³Division of Applied Mathematics, Brown University, Providence, RI 02912. E-mail: shu@dam.brown.edu. Research supported by AFOSR grant FA9550-09-1-0126 and NSF grant DMS-0809086.

⁴State Key Laboratory of Explosion Science and Technology, Beijing Institute of Technology, Beijing, 100081, P.R. China. E-mail: jgning@bit.edu.cn.

1 Introduction

Gas detonation is a supersonic flow phenomenon that consists of a precursor shock igniting a combustible mixture gas, with a thin reaction zone behind the shock. Although detonation has been studied for many years, it remains an active area of research in both theoretical studies and numerical simulations due to its practical importance. To study the gaseous detonation numerically, the governing equations could be chosen as the Euler equations describing inviscid compressible flow with the chemical reaction added. There are many difficulties in designing stable numerical schemes solving a general hyperbolic system with source terms accurately. For example, the width of reaction zone attached to the shock might be very narrow, see [3], and the source term might induce stiffness, see [9].

In this paper, we focus on how to render numerical schemes stable for gaseous detonation simulation. In practice, it is quite often to encounter situations in which the density or pressure of the numerical solutions becomes negative. For instance, highly energetic flows may contain regions with a dominant kinetic energy, and a relatively small internal energy which is easy to become negative in the simulation. Another example is the computational simulation of gas detonation propagation through different geometries. The shock diffraction may result in very low density and pressure. Under such conditions, it has been observed that numerical schemes may produce negative density or pressure, even for non-reactive gas flows, which can lead to blow-ups. This phenomenon tends to be amplified by the chemical activity. Crude replacement of negative values by positive ones not only destroys local and global conservation, but also often does not cure the instability. Therefore, it is strongly desirable to design schemes with a provable positivity-preserving property. Moreover, a conservative positivity-preserving scheme can be easily proved to be L^1 -stable.

First order and second order positivity-preserving schemes were well studied in the literature [6, 10]. So we are mainly interested in high order positivity-preserving schemes. On the one hand, low order schemes have been used in the simulation of detonation waves [12, 13], but numerical results have some deviation from the experimental results. On the other hand,

some high order schemes have been developed in recent years [5, 4, 16, 19, 20]. Successful high order numerical schemes for hyperbolic conservation laws, for example, the Runge-Kutta discontinuous Galerkin (RKDG) method in [1, 2], the essentially non-oscillatory (ENO) finite volume and finite difference schemes in [7, 17], and the weighted ENO (WENO) finite volume and finite difference schemes in [11, 8], do not automatically satisfy a strict positivity-preserving property. In fact, they may all fail for very demanding low density or low pressure test cases. Special treatments for different schemes may lead to positivity-preserving and conservation, but it is very difficult to simultaneously also maintain high order accuracy for smooth solutions with such treatments. Constructing high order schemes which automatically preserve the positivity of density and pressure is highly nontrivial. In [22, 23], two of the authors proposed an arbitrarily high order positivity-preserving Runge-Kutta discontinuous Galerkin method for compressible Euler equations, which were extensions and applications of [21, 15]. The main idea is to find some straightforward sufficient condition for the DG method of any spatial order of accuracy with first order Euler forward time discretization to keep positivity. A simple limiter which is easy and inexpensive to implement will enforce the sufficient condition without destroying conservation and accuracy. Strong stability preserving (SSP) high order Runge-Kutta or multi-step methods [17, 18] will still keep the positivity since they are convex combinations of Euler forward. With this limiter, high order RKDG methods will be positivity-preserving of density and pressure during the time evolution.

We will show an extension of this method to Euler system with an Arrhenius form of chemical reaction source term and an additional equation for the evolution of the reaction rate, which are typical governing equations for modeling the gaseous detonation. Besides density and pressure, our scheme can also maintain the positivity of the reaction rate, which is crucial to the stability of schemes in this model. We also propose a more robust implementation of the positivity-preserving limiter. The DG scheme with this new positivity-preserving limiter is stable even for very strong shocks without the need of additional TVB limiters. Extensive numerical tests of the third order DG method are reported to demonstrate the

effectiveness of our scheme.

2 Positivity-preserving high order discontinuous Galerkin method for two-dimensional reactive Euler equations

2.1 Preliminaries

We consider the dimensionless two-dimensional compressible Euler equations with a source term representing chemical reactions for the ideal gas,

$$\mathbf{w}_t + \mathbf{f}(\mathbf{w})_x + \mathbf{g}(\mathbf{w})_y = \mathbf{s}(\mathbf{w}), \quad t \geq 0, (x, y) \in \mathbb{R}^2, \quad (2.1)$$

$$\mathbf{w} = \begin{pmatrix} \rho \\ m \\ n \\ E \\ \rho Y \end{pmatrix}, \quad \mathbf{f}(\mathbf{w}) = \begin{pmatrix} m \\ \rho u^2 + p \\ \rho uv \\ (E + p)u \\ \rho u Y \end{pmatrix}, \quad \mathbf{g}(\mathbf{w}) = \begin{pmatrix} n \\ \rho uv \\ \rho v^2 + p \\ (E + p)v \\ \rho v Y \end{pmatrix}, \quad \mathbf{s}(\mathbf{w}) = \begin{pmatrix} 0 \\ 0 \\ 0 \\ 0 \\ \omega \end{pmatrix} \quad (2.2)$$

with

$$m = \rho u, \quad n = \rho v, \quad E = \frac{1}{2}\rho u^2 + \frac{1}{2}\rho v^2 + \frac{p}{\gamma - 1} + \rho q Y,$$

where q is the heat release of reaction, γ is the specific heat ratio and Y denotes the reactant mass fraction. The source term is assumed to be in an Arrhenius form

$$\omega = -\tilde{K} \rho Y e^{-\tilde{T}/T},$$

where $T = \frac{p}{\rho}$ is the temperature, \tilde{T} is the activation temperature and \tilde{K} is a constant. The eigenvalues of the Jacobian $\mathbf{f}'(\mathbf{w})$ are $u - c, u, u, u, u + c$ and the eigenvalues of the Jacobian $\mathbf{g}'(\mathbf{w})$ are $v - c, v, v, v, v + c$, where $c = \sqrt{\gamma \frac{p}{\rho}}$.

We define the set of admissible states by

$$G = \left\{ \mathbf{w} = \begin{pmatrix} \rho \\ m \\ n \\ E \\ \rho Y \end{pmatrix} \middle| \rho > 0 \quad \text{and} \quad p(\mathbf{w}) \geq 0, \quad Y \geq 0 \right\},$$

then G is a convex set since p is a concave function of \mathbf{w} . We are interested in schemes for (2.1) producing the numerical solutions in the admissible set G . We start with the

one-dimensional non-reactive equation $\mathbf{w}_t + \mathbf{f}(\mathbf{w})_x = \mathbf{0}$ and the first order Lax-Friedrichs scheme

$$\mathbf{w}_j^{n+1} = \mathbf{w}_j^n - \lambda[\widehat{\mathbf{f}}(\mathbf{w}_j^n, \mathbf{w}_{j+1}^n) - \widehat{\mathbf{f}}(\mathbf{w}_{j-1}^n, \mathbf{w}_j^n)], \quad (2.3)$$

$$\widehat{\mathbf{f}}(\mathbf{u}, \mathbf{v}) = \frac{1}{2}[\mathbf{f}(\mathbf{u}) + \mathbf{f}(\mathbf{v}) - a(\mathbf{v} - \mathbf{u})], \quad a = \|(|u| + c)\|_\infty, \quad (2.4)$$

where n refers to the time step and j to the spatial cell, and $\lambda = \frac{\Delta t}{\Delta x}$ is the ratio of time and space mesh sizes. Following Remark 2.4 in [22], it is easy to check that, for the scheme (2.3), $\mathbf{w}_j^n, \mathbf{w}_{j\pm 1}^n \in G$ implies $\mathbf{w}_j^{n+1} \in G$ under the CFL condition $\lambda a \leq 1$. Other examples of positivity preserving fluxes include the Godunov flux, the Boltzmann type flux [14], and the HLLE flux, which may all be used in our framework.

2.2 Discontinuous Galerkin method

We review the formulation of the DG method in [2] briefly. Assume T_h is a triangulation of the spatial domain Ω . For simplicity, we use \mathbf{x} to denote (x, y) and $d\mathbf{x}$ to denote $dx dy$ in this subsection. For each $t \geq 0$, we seek the approximation $\mathbf{w}_h(\mathbf{x}, t)$ in the piecewise polynomial space

$$V_h = \{v_h \in L^\infty(\Omega) : v_h|_K \in P^k(K), \forall K \in T_h\},$$

where P^k denotes all the polynomials of degree k . The weak formulation of DG method solving (2.1) is, find $\mathbf{w}_h \in V_h$ satisfying, $\forall v_h \in V_h$,

$$\frac{d}{dt} \int_K \mathbf{w}_h v_h d\mathbf{x} + \sum_{e \in \partial K} \int_e \mathbf{h}_{K,e}(\mathbf{w}_h^{int(K)}, \mathbf{w}_h^{ext(K)}, \nu_{e,K}) v_h d\Gamma - \int_K \mathbf{F}(\mathbf{w}_h) \cdot \nabla v_h d\mathbf{x} = \int_k \mathbf{s}(\mathbf{w}_h) v_h d\mathbf{x}, \quad (2.5)$$

where $\mathbf{F} = \langle \mathbf{f}, \mathbf{g} \rangle$, $\nu_{e,K}$ is the outward normal vector of the edge e on the element K . The superscripts “ $int(K)$ ” and “ $ext(K)$ ” refer to values of the solution from inside the element K and outside the element K (or inside the neighboring element K'). The consistent numerical flux satisfies $\mathbf{h}_{K,e}(\mathbf{u}, \mathbf{v}, \nu) = -\mathbf{h}_{K',e}(\mathbf{v}, \mathbf{u}, -\nu)$ where K' is the neighboring element sharing the edge e with the element K . We will drop the subscripts “ K, e ” from the flux \mathbf{h} when it does not cause confusion. We consider the Lax-Friedrichs flux as an example throughout

the rest of this paper,

$$\mathbf{h}(\mathbf{u}, \mathbf{v}, \nu) = \frac{1}{2}[\mathbf{F}(\mathbf{u}) \cdot \nu + \mathbf{F}(\mathbf{v}) \cdot \nu - a(\mathbf{v} - \mathbf{u})], \quad a = \|(|\langle u, v \rangle| + c)\|_\infty.$$

Except the first integral (which is evaluated exactly), the integrals in (2.5) can be approximated by proper quadrature rules. Time discretizations can be achieved by the strong stability preserving (also called TVD) Runge-Kutta or multi-step time discretizations. See [2] for more details.

To construct conservative positivity-preserving schemes, the most important step is to achieve positivity for the cell averages. We only need to discuss Euler forward time discretization because high order SSP time discretizations are convex combinations of Euler forward thus will keep the positivity due to the convexity of G . Taking the test function as $v_h = 1$ in (2.5), we get the scheme satisfied by the cell averages in the DG method. Consider the Euler forward time discretization,

$$\frac{|K|}{\Delta t}(\overline{\mathbf{w}}_K^{n+1} - \overline{\mathbf{w}}_K^n) + \sum_{e \in \partial K} \int_e \mathbf{h}(\mathbf{w}_h^{int(K)}, \mathbf{w}_h^{ext(K)}, \nu_e) d\Gamma = \int_K \mathbf{s}(\mathbf{w}_h) dx, \quad (2.6)$$

where $\overline{\mathbf{w}}_K^n$ denotes the cell average of \mathbf{w}_h on K at time level n and $|K|$ is the area of K .

2.3 Rectangular meshes

For simplicity we assume we have a uniform rectangular mesh. At time level n , we have the DG polynomials of degree k , $\mathbf{w}_{ij}(x, y) = (\rho_{ij}(x, y), m_{ij}(x, y), n_{ij}(x, y), E_{ij}(x, y), \rho Y_{ij}(x, y))^T$ with the cell average $\overline{\mathbf{w}}_{ij}^n$ on the (i, j) cell $[x_{i-\frac{1}{2}}, x_{i+\frac{1}{2}}] \times [y_{j-\frac{1}{2}}, y_{j+\frac{1}{2}}]$. Let $\mathbf{w}_{i-\frac{1}{2}, j}^+(y)$, $\mathbf{w}_{i+\frac{1}{2}, j}^-(y)$, $\mathbf{w}_{i, j-\frac{1}{2}}^+(x)$, $\mathbf{w}_{i, j+\frac{1}{2}}^-(x)$ denote the traces of $\mathbf{w}_{ij}(x, y)$ on the four edges respectively.

Assume that we use a L -point Gauss quadrature for the line integral and tensor of two one-dimensional L -point Gauss quadratures for the double integral in (2.6) where $L \geq k + 1$ (see [2] for an analysis of the requirement of the numerical quadrature for the accuracy of the DG solution). Let $S_i^x = \{x_i^\beta : \beta = 1, \dots, L\}$ denote the Gauss quadrature points on $[x_{i-\frac{1}{2}}, x_{i+\frac{1}{2}}]$, and $S_j^y = \{y_j^\beta : \beta = 1, \dots, L\}$ denote the Gauss quadrature points on $[y_{j-\frac{1}{2}}, y_{j+\frac{1}{2}}]$. For instance, $(x_{i-\frac{1}{2}}, y_j^\beta)$ ($\beta = 1, \dots, L$) are the Gauss quadrature points on the

left edge of the (i, j) cell. The subscript β will denote the values at the Gauss quadrature points, for instance, $\mathbf{w}_{i-\frac{1}{2},\beta}^+ = \mathbf{w}_{i-\frac{1}{2},j}^+(y_j^\beta)$. Also, w_β denotes the corresponding quadrature weight on the interval $[-\frac{1}{2}, \frac{1}{2}]$, so that $\sum_{\beta=1}^L w_\beta = 1$. We also need to use the N -point Gauss-Lobatto quadrature rule where N is the smallest integer such that $2N - 3 \geq k$, and we distinguish the two quadrature rules by adding hats to the Gauss-Lobatto points, i.e., $\widehat{S}_i^x = \{\widehat{x}_i^\alpha : \alpha = 1, \dots, N\}$ will denote the Gauss-Lobatto quadrature points on $[x_{i-\frac{1}{2}}, x_{i+\frac{1}{2}}]$, and $\widehat{S}_j^y = \{\widehat{y}_j^\alpha : \alpha = 1, \dots, N\}$ will denote the Gauss-Lobatto quadrature points on $[y_{j-\frac{1}{2}}, y_{j+\frac{1}{2}}]$.

Then (2.6) becomes

$$\begin{aligned} \overline{\mathbf{w}}_{ij}^{n+1} &= \overline{\mathbf{w}}_{ij}^n - \lambda_1 \sum_{\beta=1}^L w_\beta \left[\mathbf{h}_1 \left(\mathbf{w}_{i+\frac{1}{2},\beta}^-, \mathbf{w}_{i+\frac{1}{2},\beta}^+ \right) - \mathbf{h}_1 \left(\mathbf{w}_{i-\frac{1}{2},\beta}^-, \mathbf{w}_{i-\frac{1}{2},\beta}^+ \right) \right] \\ &\quad - \lambda_2 \sum_{\beta=1}^L w_\beta \left[\mathbf{h}_2 \left(\mathbf{w}_{\beta,j+\frac{1}{2}}^-, \mathbf{w}_{\beta,j+\frac{1}{2}}^+ \right) - \mathbf{h}_2 \left(\mathbf{w}_{\beta,j-\frac{1}{2}}^-, \mathbf{w}_{\beta,j-\frac{1}{2}}^+ \right) \right] \\ &\quad + \Delta t \sum_{\alpha=1}^L \sum_{\beta=1}^L w_\alpha w_\beta \mathbf{s}(\mathbf{w}(x_i^\alpha, y_j^\beta)) \end{aligned} \quad (2.7)$$

where $\lambda_1 = \frac{\Delta t}{\Delta x}$, $\lambda_2 = \frac{\Delta t}{\Delta y}$ and

$$\mathbf{h}_1(\mathbf{u}, \mathbf{v}) = \frac{1}{2} [\mathbf{f}(\mathbf{u}) + \mathbf{f}(\mathbf{v}) - a(\mathbf{v} - \mathbf{u})]$$

$$\mathbf{h}_2(\mathbf{u}, \mathbf{v}) = \frac{1}{2} [\mathbf{g}(\mathbf{u}) + \mathbf{g}(\mathbf{v}) - a(\mathbf{v} - \mathbf{u})].$$

We use \otimes to denote the tensor product, for instance, $S_i^x \otimes S_j^y = \{(x, y) : x \in S_i^x, y \in S_j^y\}$.

Define the set S_{ij} as

$$S_{ij} = (S_i^x \otimes \widehat{S}_j^y) \cup (\widehat{S}_i^x \otimes S_j^y) \cup (S_i^x \otimes S_j^y). \quad (2.8)$$

Theorem 2.1. *If the DG polynomial $\mathbf{w}_{ij}(x, y) \in G$, $\forall (x, y) \in S_{ij}$, then the scheme (2.7) is positivity-preserving, namely, $\overline{\mathbf{w}}_{ij}^{n+1} \in G$ under the time step restriction*

$$a(\lambda_1 + \lambda_2) \leq \frac{1}{2} \widehat{w}_1, \quad \max \left\{ \Delta t \widetilde{K} e^{-\widetilde{T}/T} \right\} \leq \frac{1}{2},$$

where the maximum is taken over $S_i^x \otimes S_j^y$ for all the rectangles.

Proof. We can rewrite (2.6) as $\mathbf{w}_{ij}^{n+1} = \frac{1}{2}\mathbf{C} + \frac{1}{2}\mathbf{S}$ where

$$\begin{aligned} \mathbf{C} = & \bar{\mathbf{w}}_{ij}^n - 2\lambda_1 \sum_{\beta=1}^L w_\beta \left[\mathbf{h}_1 \left(\mathbf{w}_{i+\frac{1}{2},\beta}^-, \mathbf{w}_{i+\frac{1}{2},\beta}^+ \right) - \mathbf{h}_1 \left(\mathbf{w}_{i-\frac{1}{2},\beta}^-, \mathbf{w}_{i-\frac{1}{2},\beta}^+ \right) \right] \\ & - 2\lambda_2 \sum_{\beta=1}^L w_\beta \left[\mathbf{h}_2 \left(\mathbf{w}_{\beta,j+\frac{1}{2}}^-, \mathbf{w}_{\beta,j+\frac{1}{2}}^+ \right) - \mathbf{h}_2 \left(\mathbf{w}_{\beta,j-\frac{1}{2}}^-, \mathbf{w}_{\beta,j-\frac{1}{2}}^+ \right) \right] \end{aligned}$$

and

$$\mathbf{S} = \bar{\mathbf{w}}_{ij}^n + 2\Delta t \sum_{\alpha=1}^L \sum_{\beta=1}^L w_\alpha w_\beta \mathbf{s}(\mathbf{w}(x_i^\alpha, y_j^\beta)).$$

By Theorem 3.1 in [22], we have $\mathbf{C} \in G$. So it suffices to prove $\mathbf{S} \in G$. Gauss quadrature rule implies

$$\bar{\mathbf{w}}_{ij}^n = \sum_{\alpha=1}^L \sum_{\beta=1}^L w_\alpha w_\beta \mathbf{w}(x_i^\alpha, y_j^\beta). \quad (2.9)$$

Thus,

$$\mathbf{S} = \sum_{\alpha=1}^L \sum_{\beta=1}^L w_\alpha w_\beta \left[\mathbf{w}(x_i^\alpha, y_j^\beta) + 2\Delta t \mathbf{s}(\mathbf{w}(x_i^\alpha, y_j^\beta)) \right]$$

Given $\mathbf{w} \in G$, then it is easy to check that $\mathbf{w} + 2\Delta t \mathbf{s}(\mathbf{w}) \in G$ if $\Delta t \tilde{K} e^{-\tilde{T}/T} \leq \frac{1}{2}$. So $\mathbf{S} \in G$. \square

Remark 2.1. *The result can be extended to a general equation of state or other types of reaction rate (for instance, the Heaviside form) by following [23].*

2.4 Triangular meshes

For each triangle K we denote by l_K^i ($i = 1, 2, 3$) the length of its three edges e_K^i ($i = 1, 2, 3$), with outward unit normal vector ν^i ($i = 1, 2, 3$). Assume the line integrals in (2.6) are solved by the L -point Gauss quadrature where $L \geq k + 1$, and the source integral is solved by a M -point quadrature on a triangle with positive weights (for instance, 7-point quadrature should be used for P^2 element, see [2] for more details) in which \mathbf{x}_K^γ and \tilde{w}_γ denote the quadrature points and normalized weights with $\sum_{\gamma=1}^M \tilde{w}_\gamma = 1$.

Then (2.6) becomes

$$\bar{\mathbf{w}}_K^{n+1} = \bar{\mathbf{w}}_K^n - \frac{\Delta t}{|K|} \sum_{i=1}^3 \sum_{\beta=1}^L \mathbf{h}(\mathbf{w}_{i,\beta}^{int(K)}, \mathbf{w}_{i,\beta}^{ext(K)}, \nu^i) w_\beta l_K^i + \Delta t \sum_{\gamma=1}^M \tilde{w}_\gamma \mathbf{s}(\mathbf{w}(\mathbf{x}_K^\gamma)). \quad (2.10)$$

We need a special quadrature on a triangle introduced in [24]. In the barycentric coordinates, the set S_K^k of quadrature points for polynomials of degree k on a triangle K can be written as

$$S_K^k = \left\{ \begin{aligned} &\left(\frac{1}{2} + v^\beta, \left(\frac{1}{2} + \widehat{u}^\alpha \right) \left(\frac{1}{2} - v^\beta \right), \left(\frac{1}{2} - \widehat{u}^\alpha \right) \left(\frac{1}{2} - v^\beta \right) \right), \\ &\left(\left(\frac{1}{2} - \widehat{u}^\alpha \right) \left(\frac{1}{2} - v^\beta \right), \frac{1}{2} + v^\beta, \left(\frac{1}{2} + \widehat{u}^\alpha \right) \left(\frac{1}{2} - v^\beta \right) \right), \\ &\left(\left(\frac{1}{2} + \widehat{u}^\alpha \right) \left(\frac{1}{2} - v^\beta \right), \left(\frac{1}{2} - \widehat{u}^\alpha \right) \left(\frac{1}{2} - v^\beta \right), \frac{1}{2} + v^\beta \right) \end{aligned} \right\} \quad (2.11)$$

where \widehat{u}^α ($\alpha = 1, \dots, N$) and v^β ($\beta = 1, \dots, L$) are the Gauss-Lobatto and Gauss quadrature points on the interval $[-\frac{1}{2}, \frac{1}{2}]$ respectively. Define S_K as the union of S_K^k and the M -point quadrature on the triangle K . Following Theorem 5.1 in [24] and Theorem 2.1, we have

Theorem 2.2. *If the DG polynomial $\mathbf{w}_K(x, y) \in G$, $\forall (x, y) \in S_K$, then the scheme (2.10) is positivity-preserving, namely, $\overline{\mathbf{w}}_K^{n+1} \in G$ under the time step restriction*

$$a \frac{\Delta t}{|K|} \sum_{i=1}^3 l_K^i \leq \frac{1}{3} \widehat{w}_1, \quad \max \left\{ \Delta t \widetilde{K} e^{-\widetilde{T}/T} \right\} \leq \frac{1}{2},$$

where the maximum is taken over \mathbf{x}_K^γ , $\gamma = 1, \dots, M$ for all the triangles.

2.5 L^1 stability

The limiter in [22] can be used to enforce the conditions in Theorem 2.1 and Theorem 2.2. We will describe an improved implementation of this limiter in the next section.

With the limiter added, the full high order DG scheme will keep density, pressure and reactant mass fraction non-negative in the mean during the time evolution.

Theorem 2.3. *Assuming vanishing, reflective or periodic boundary conditions, suppose the DG polynomial satisfies $\mathbf{w}_K(\mathbf{x}) \in G$, $\forall \mathbf{x} \in S_K$, then the scheme (2.10) satisfies the following L^1 stability:*

$$\sum_K |\overline{\rho}_K^{n+1}| = \sum_K |\overline{\rho}_K^n|, \quad \sum_K |\overline{E}_K^{n+1}| = \sum_K |\overline{E}_K^n|, \quad \sum_K |\overline{\rho Y}_K^{n+1}| \leq \sum_K |\overline{\rho Y}_K^n|.$$

Proof. Take the summation of (2.10) for all K , then we have

$$\sum_K \bar{\mathbf{w}}_K^{n+1} = \sum_K \bar{\mathbf{w}}_K^n + \Delta t \sum_K \sum_{\gamma=1}^M \tilde{w}_\gamma \mathbf{s}(\mathbf{w}(\mathbf{x}_K^\gamma)).$$

The first component reads $\sum_K \bar{\rho}_K^{n+1} = \sum_K \bar{\rho}_K^n$. Theorem (2.2) and (2.9) imply that $\bar{\mathbf{w}}_K^{n+1}$, $\bar{\mathbf{w}}_K^{n+1} \in G$, thus $\bar{\rho}_K^{n+1}, \bar{\rho}_K^n \geq 0$. Therefore, $\sum_K |\bar{\rho}_K^{n+1}| = \sum_K |\bar{\rho}_K^n|$. Similarly, we get $\sum_K |\bar{E}_K^{n+1}| = \sum_K |\bar{E}_K^n|$. Notice that the fifth component of $\mathbf{s}(\mathbf{w}(\mathbf{x}_K^\gamma))$ is non-positive, which leads to the last inequality. \square

3 An improved implementation of the positivity-preserving limiter

3.1 Positivity-preserving limiter

At the time level n , given the DG polynomial $\mathbf{w}_K(\mathbf{x})$ with the cell average $\bar{\mathbf{w}}_K \in G$, we would like to modify it into another polynomial

$$\tilde{\mathbf{w}}_K(\mathbf{x}) = \theta_K(\mathbf{w}_K(\mathbf{x}) - \bar{\mathbf{w}}_K) + \bar{\mathbf{w}}_K \quad (3.1)$$

where $\theta_K \in [0, 1]$ is to be determined, such that $\tilde{\mathbf{w}}_K(\mathbf{x}) \in G, \forall \mathbf{x} \in S_K$. If θ_K is the largest such number (the smallest one is $\theta_K = 0$), then this limiter will not destroy accuracy for smooth solutions, see [22]. Following [22], it can be implemented as:

1. First, enforce the positivity of density (and reactant mass fraction). Pick a small number ε such that $\bar{\rho}_K \geq \varepsilon$ for all K . In practice, we can choose $\varepsilon = 10^{-13}$. For each element K , compute

$$\hat{\rho}_K(\mathbf{x}) = \theta_K^1 [\rho_K(\mathbf{x}) - \bar{\rho}_K] + \bar{\rho}_K, \quad \theta_K^1 = \min_{\mathbf{x} \in S_K} \left\{ 1, \left| \frac{\bar{\rho}_K - \varepsilon}{\bar{\rho}_K - \rho_K(\mathbf{x})} \right| \right\}, \quad (3.2)$$

$$\hat{\rho Y}_K(\mathbf{x}) = \theta_K^2 [\rho Y_K(\mathbf{x}) - \bar{\rho Y}_K] + \bar{\rho Y}_K, \quad \theta_K^2 = \min_{\mathbf{x} \in S_K} \left\{ 1, \left| \frac{\bar{\rho Y}_K}{\bar{\rho Y}_K - \rho Y_K(\mathbf{x})} \right| \right\}. \quad (3.3)$$

2. Second, enforce the positivity of pressure. Define $\hat{\mathbf{w}}_K = (\hat{\rho}_K, m_K, n_K, E_K, \hat{\rho Y}_K)^T$. For each $\mathbf{x} \in S_K$, if $p(\hat{\mathbf{w}}_K(\mathbf{x})) \geq 0$ define $\theta_{\mathbf{x}} = 1$; otherwise, define $\theta_{\mathbf{x}}$ as the solution of

$$p(\theta_{\mathbf{x}}(\hat{\mathbf{w}}_K(\mathbf{x}) - \bar{\mathbf{w}}_K) + \bar{\mathbf{w}}_K) = 0. \quad (3.4)$$

Then get the limited polynomial

$$\tilde{\mathbf{w}}_K(\mathbf{x}) = \theta_K(\widehat{\mathbf{w}}_K(\mathbf{x}) - \overline{\mathbf{w}}_K) + \overline{\mathbf{w}}_K, \quad \theta_K = \min_{\mathbf{x} \in S_K} \theta_{\mathbf{x}}. \quad (3.5)$$

Even though we only need to solve a quadratic equation of $\theta_{\mathbf{x}}$ in (3.4), in practice θ_K solved from (3.4) cannot guarantee the strict non-negativity of $p(\tilde{\mathbf{w}}_K(\mathbf{x}))$ numerically due to the round off errors for some wild data, e.g., blast waves. In [22], it was reported that for problems with very strong shocks, positivity limiter alone implemented as above may not be enough for stability, further application of a TVB limiter may be needed.

Here we propose a slightly different but very robust implementation of (3.4) so that the TVB limiter is no longer needed accordingly to our numerical tests. Notice that p is a concave function of \mathbf{w} , thus we have the Jensen's inequality

$$p(\theta(\mathbf{w} - \overline{\mathbf{w}}) + \overline{\mathbf{w}}) = p(\theta\mathbf{w} + (1-\theta)\overline{\mathbf{w}}) \geq \theta p(\mathbf{w}) + (1-\theta)p(\overline{\mathbf{w}}), \quad \text{if } \rho(\mathbf{w}) > 0, \rho(\overline{\mathbf{w}}) > 0. \quad (3.6)$$

Therefore, if $\overline{\mathbf{w}} \in G$, $\rho(\mathbf{w}) > 0$ and $p(\mathbf{w}) < 0$, then

$$\theta = \frac{p(\overline{\mathbf{w}})}{p(\overline{\mathbf{w}}) - p(\mathbf{w})} \quad (3.7)$$

satisfies that $p(\theta(\mathbf{w} - \overline{\mathbf{w}}) + \overline{\mathbf{w}}) \geq 0$. Although θ defined in (3.7) is smaller than the real solution of $p(\theta(\mathbf{w} - \overline{\mathbf{w}}) + \overline{\mathbf{w}}) = 0$, it is actually of the similar type as θ_K^1 in (3.2). It is straightforward to prove the accuracy for smooth solutions following the argument in [22].

We can formulate the new robust implementation of the limiter as, for each element K ,

1. Compute (3.2) and (3.3).
2. Define $\widehat{\mathbf{w}}_K = (\widehat{\rho}_K, m_K, n_K, E_K, \widehat{\rho Y}_K)^T$. For each $\mathbf{x} \in S_K$, if $p(\widehat{\mathbf{w}}_K(\mathbf{x})) \geq 0$ set $\theta_{\mathbf{x}} = 1$; otherwise, set

$$\theta_{\mathbf{x}} = \frac{p(\overline{\mathbf{w}}_K)}{p(\overline{\mathbf{w}}_K) - p(\widehat{\mathbf{w}}_K(\mathbf{x}))}.$$

Then get the limited polynomial (3.5).

3.2 The algorithm for SSP Runge-Kutta time discretizations

Theoretically, there is a complication regarding the time step restriction in Theorem 2.1 and Theorem 2.2 for a Runge-Kutta time discretization. Consider the third order SSP Runge-Kutta method. To enforce the CFL condition rigorously, we need to get an accurate estimation of $a = \max_{\mathbf{x} \in S_K} (|\langle u, v \rangle| + c)$ for all the three stages based only on the numerical solution at time level n , which is highly nontrivial mathematically. An efficient solution is, if a preliminary calculation to the next time step produces negative density or pressure, then recalculate from the time step n with half the previous time step. This complication does not exist if we use a SSP multi-step time discretization.

The algorithm flow chart for the third order SSP Runge-Kutta method on triangular meshes is

1. Given the DG polynomials $\mathbf{w}_K(\mathbf{x})$ at time step n satisfying the cell average $\bar{\mathbf{w}}_K^n \in G$ and $\mathbf{w}_K(\mathbf{x}) \in G, \forall \mathbf{x} \in S_K$, calculate $a = \max_{\mathbf{x} \in S_K} (|\langle u, v \rangle| + c)$, $b = \max_{\mathbf{x} \in S_K} \tilde{K} e^{-\tilde{T}/T}$ where the maximum is taken over S_K for all K . Set the time step

$$\Delta t = \min \left\{ \frac{1}{3} \frac{\hat{w}_1 |K|}{a \sum_{i=1}^3 l_K^i}, \frac{1}{2b} \right\}.$$

2. Calculate the first stage with $\mathbf{w}_K(\mathbf{x})$. Let $\mathbf{w}_K^1(\mathbf{x})$ denote the solution of the first stage. Modify it by the limiter (3.5) into $\tilde{\mathbf{w}}_K^1(\mathbf{x})$.
3. Calculate the second stage with $\tilde{\mathbf{w}}_K^1(\mathbf{x})$. Let $\mathbf{w}_K^2(\mathbf{x})$ denote the solution of the second stage. If its cell average is not in G (by Theorem 2.2, this means that a or b calculated based on $\mathbf{w}_K(\mathbf{x})$ is smaller than the ones of $\tilde{\mathbf{w}}_K^1(\mathbf{x})$), then go back to step two and restart with half time step; otherwise, modify it by the limiter (3.5) into $\tilde{\mathbf{w}}_K^2(\mathbf{x})$.
4. Calculate the third stage with $\tilde{\mathbf{w}}_K^2(\mathbf{x})$. Let $\mathbf{w}_K^3(\mathbf{x})$ denote the solution of the third stage. If its cell average is not in G (by Theorem 2.2, this means that a or b calculated based on $\mathbf{w}_K(\mathbf{x})$ is smaller than the ones of $\tilde{\mathbf{w}}_K^2(\mathbf{x})$), then go back to step two and restart with half time step; otherwise, modify it by the limiter (3.5) into $\tilde{\mathbf{w}}_K^3(\mathbf{x})$.

4 Numerical Tests

4.1 Euler equations

We test the robustness of the new implementation of the positivity-preserving limiter for non-reactive Euler equations by using the algorithm in the previous section.

In [1, 2], the TVB limiter was used to kill oscillations for high order DG schemes solving Euler equations with strong shocks. For smooth solutions, the TVB limiter will not destroy the accuracy. However, TVB limiter is not sufficient for stabilizing high order schemes solving Euler equations when low density or low pressure emerges. In [22, 24, 23], the third order DG scheme with TVB limiter and positivity-preserving limiter performed very well for all test cases for which DG method with only TVB limiter will blow up due to the presence of negative density or negative pressure.

By the following numerical tests, we will see that the positivity-preserving limiter itself can stabilize the high order DG schemes without the TVB limiter. We test the third order DG method and the third order SSP Runge-Kutta time discretization with only the positivity-preserving limiter (3.5), solving the one-dimensional and two-dimensional compressible Euler equations for ideal gas with $\gamma = 1.4$.

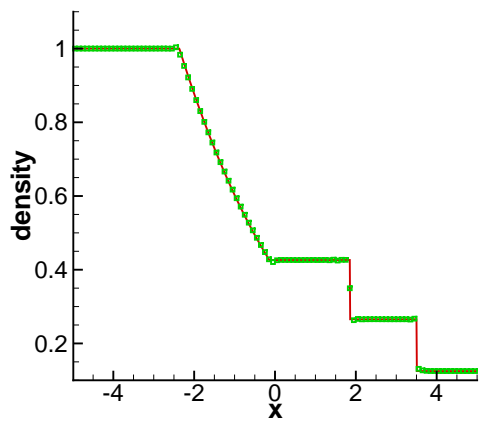
Example 4.1. *Shock tube problems.*

See Figure 4.1 for the results of Sod and Lax problems using 100 cells, which are comparable to the results of the RKDG method with the characteristicwise TVB limiter in [1].

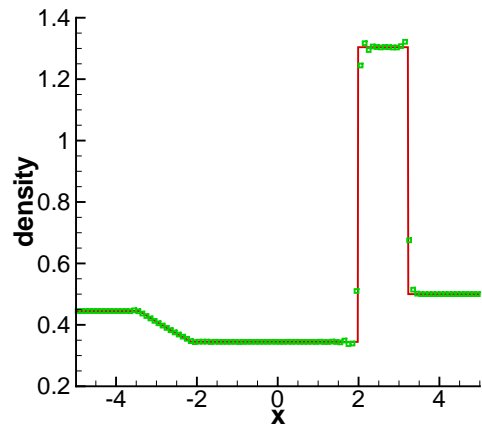
Example 4.2. *Interaction of blast waves.*

This example is the same as the one in [1]. See Figure 4.2 for the comparison of results of the two limiters. As can be expected, the TVB limiter can kill oscillations while the positivity limiter cannot, however, the positivity limiter alone will smear the discontinuity less.

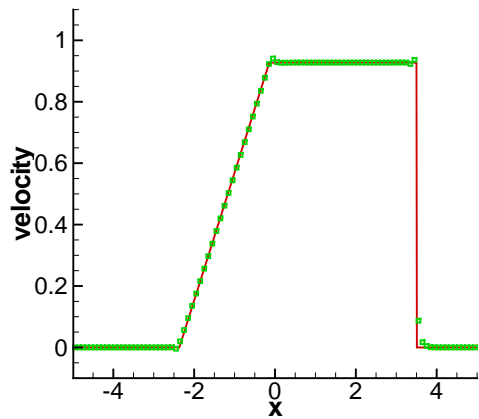
Example 4.3. *Sedov point blast.*



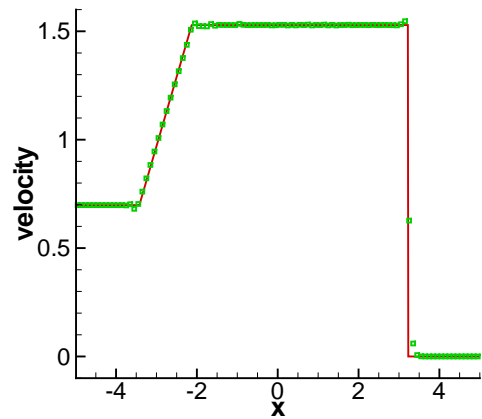
(a) Sod Problem: Density



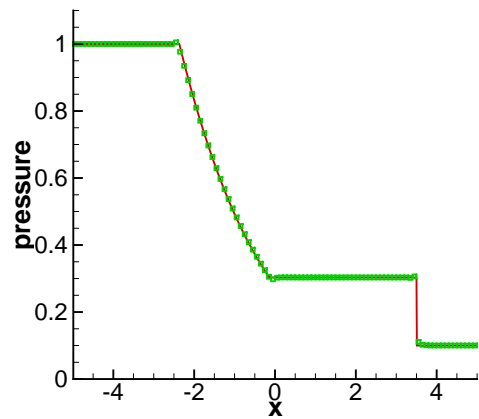
(b) Lax Problem: Density



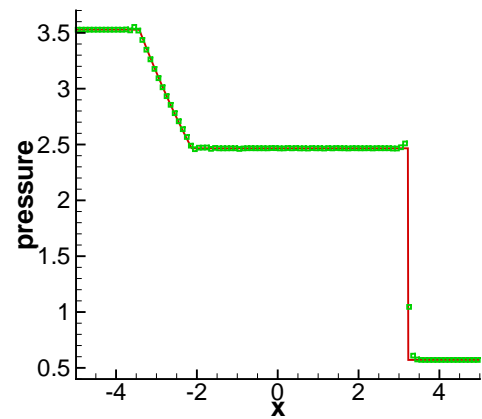
(c) Sod Problem: Velocity



(d) Lax Problem: Velocity

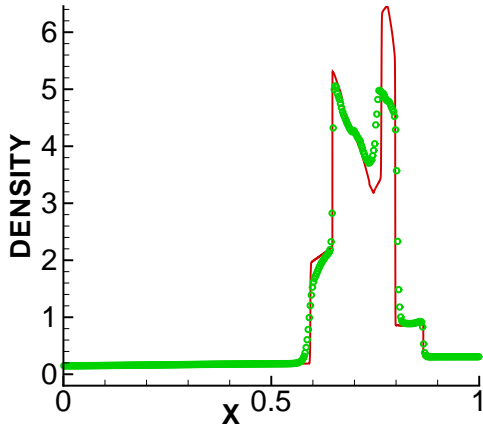


(e) Sod Problem: Pressure

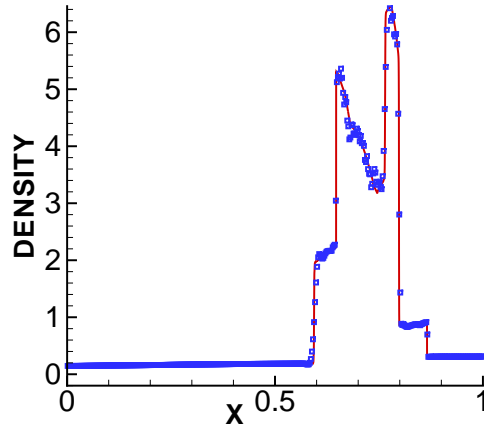


(f) Lax Problem: Pressure

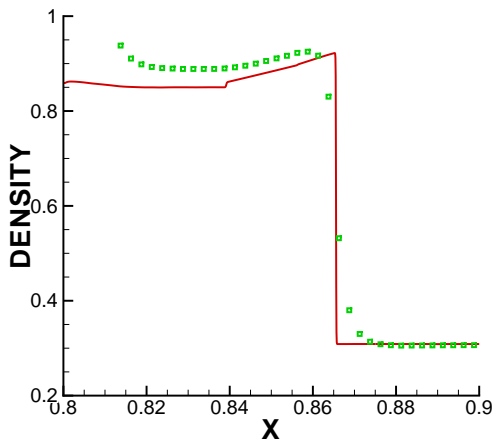
Figure 4.1: Shock tube problems. P^2 element DG with only the positivity-preserving limiter. The solid lines are the exact solutions. The symbols are the numerical solutions.



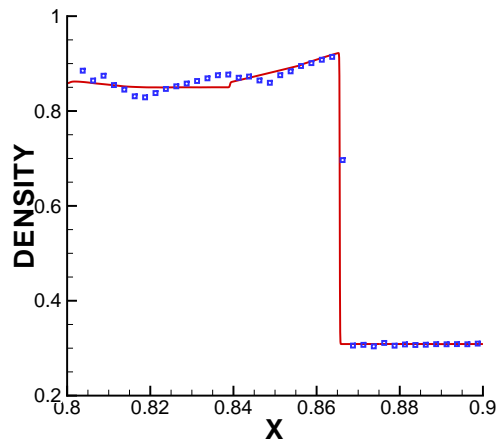
(a) Only TVB limiter



(b) Only positivity limiter



(c) Only TVB limiter (zoomed)



(d) Only positivity limiter (zoomed)

Figure 4.2: Interaction of blast waves. P^2 element DG with two different limiters on 400 cells. The solid line is computed by the fifth order WENO on a very fine mesh. The symbols are the numerical solutions.

The initial and boundary conditions are the same as in [22]. See Figure 4.3 for the result of DG with only the positivity limiter.

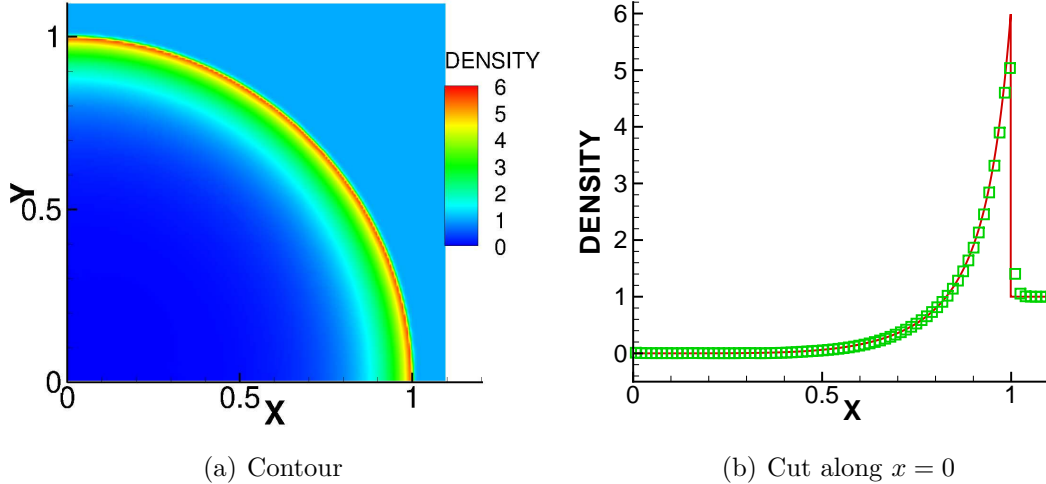


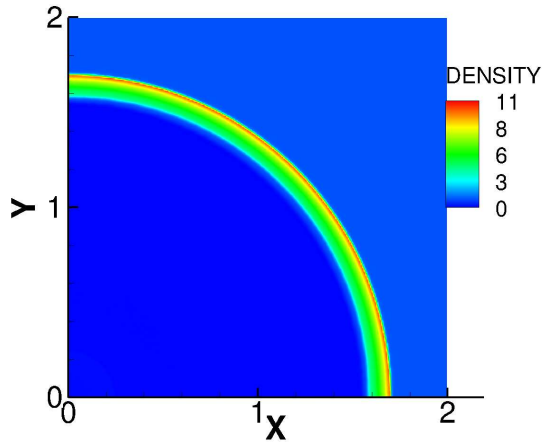
Figure 4.3: 2D Sedov Problem. P^2 element DG with only the positivity limiter on a 160×160 mesh. The solid line is the exact solution.

4.2 The reactive Euler equations

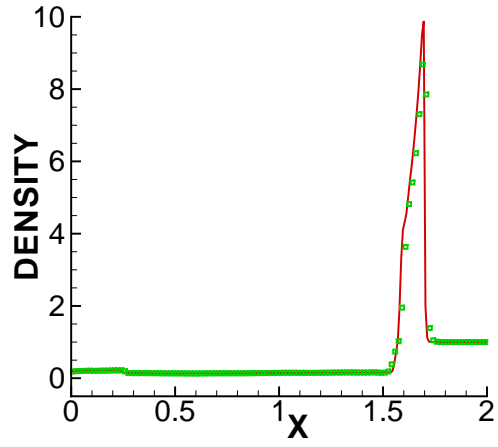
In this subsection, we show the test results for the third order RKDG method with only the positivity-preserving limiter solving (2.1). The parameters are $\gamma = 1.2$, $q = 50$, $\tilde{T} = 50$, $\tilde{K} = 2566.4$. For all the test cases in this subsection, the RKDG method with only TVB limiter may blow up at a certain time.

Example 4.4. *Numerical convergence study.*

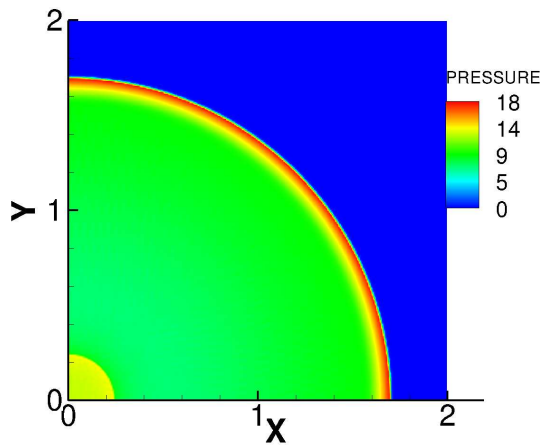
We test the numerical (grid) convergence of our scheme in this example. The domain is $[0, 2] \times [0, 2]$. The initial condition is, if $x^2 + y^2 \leq 0.36$, then $(\rho, u, v, p, Y) = (1, 0, 0, 80, 0)$; otherwise, $(\rho, u, v, p, Y) = (1, 0, 0, 10^{-9}, 1)$. The boundary conditions for the bottom and the left are reflective. The terminal time is $t = 0.2$. The mesh is uniformly rectangular. See the comparison of results of $\Delta x = \Delta y = \frac{1}{60}$ and $\Delta x = \Delta y = \frac{1}{120}$ in Figure 4.4. We observe good grid convergence on these two meshes.



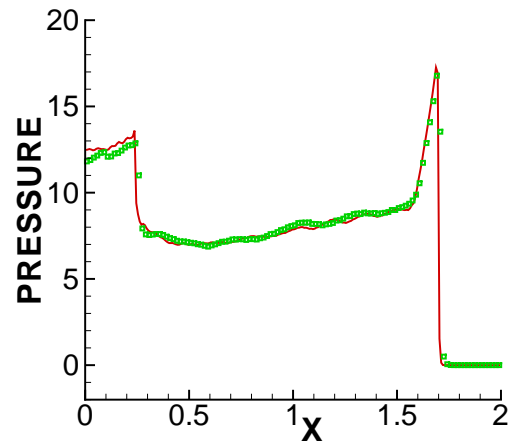
(a) Contour of density



(b) Cut along $y = 0$



(c) Contour of pressure



(d) Cut along $y = 0$

Figure 4.4: Convergence study. The colored contour and the solid line on the right are the results of $\Delta x = \Delta y = \frac{1}{120}$. The symbols on the right denote the result of $\Delta x = \Delta y = \frac{1}{60}$.

Example 4.5. *Detonation diffraction problems.*

The simulation of gaseous detonation waves through different geometries is numerically challenging especially for the high order schemes mainly because the pressure or density may drop very close to zero when the shock wave is diffracted. Here we test the detonation diffraction at three different angles.

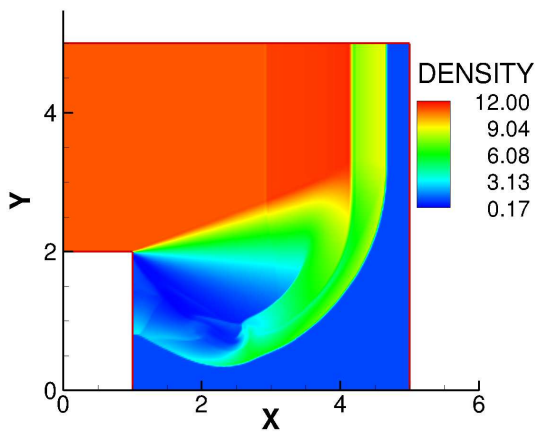
The first one is ninety degrees. The initial conditions are, if $x < 0.5$, $(\rho, u, v, E, Y) = (11, 6.18, 0, 970, 1)$; otherwise, $(\rho, u, v, E, Y) = (1, 0, 0, 55, 1)$. The boundary conditions are reflective except that at $x = 0$, $(\rho, u, v, E, Y) = (11, 6.18, 0, 970, 1)$. The terminal time is $t = 0.6$. The mesh is uniformly rectangular. See Figure 4.5 for the result of $\Delta x = \Delta y = \frac{1}{48}$.

The second one is one hundred and twenty degrees. The initial conditions are, if $x < 0.6$ and $y \geq 2$, $(\rho, u, v, E, Y) = (11, 6.18, 0, 970, 1)$; otherwise, $(\rho, u, v, E, Y) = (1, 0, 0, 55, 1)$. The boundary conditions are reflective except that at $x = 0$, $(\rho, u, v, E, Y) = (11, 6.18, 0, 970, 1)$. The terminal time is $t = 0.68$. The mesh is nonuniform, mixed with rectangles and triangles. See Figure 4.6(a) for the illustration of the mesh. See Figure 4.7 for the result where the length of the smallest edge in the mesh is $\frac{1}{32\sqrt{3}}$.

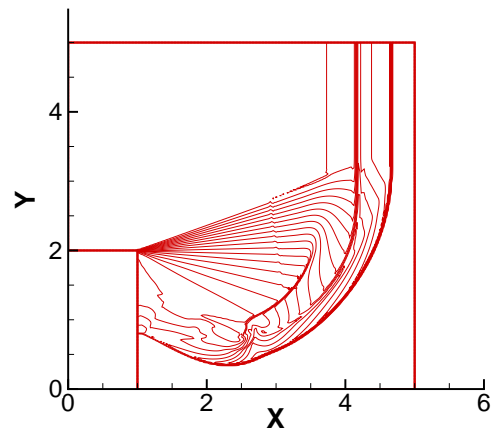
The third one is one hundred and thirty-five degrees. The initial conditions are, if $x < 1.5$ and $y \geq 2$, $(\rho, u, v, E, Y) = (11, 6.18, 0, 970, 1)$; otherwise, $(\rho, u, v, E, Y) = (1, 0, 0, 55, 1)$. The boundary conditions are reflective except that at $x = 0$, $(\rho, u, v, E, Y) = (11, 6.18, 0, 970, 1)$. The terminal time is $t = 0.68$. The mesh is uniform, mixed with rectangles and triangles. See Figure 4.6(b) for the illustration of the mesh. See Figure 4.8 for the result of the mesh size $\frac{1}{24}$.

Example 4.6. *Multiple obstacles.*

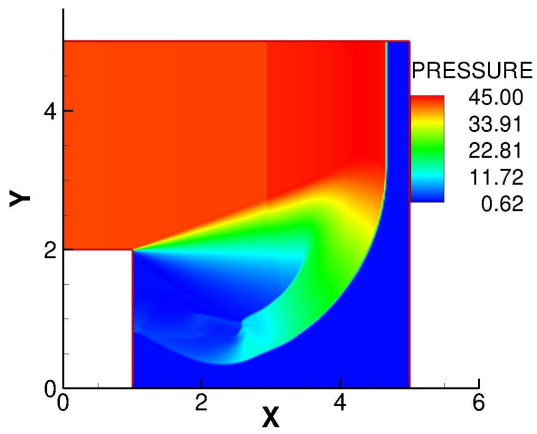
The initial condition is, if $x^2 + y^2 \leq 0.36$, then $(\rho, u, v, E, Y) = (7, 0, 0, 200, 0)$; otherwise, $(\rho, u, v, E, Y) = (1, 0, 0, 55, 1)$. The boundary conditions are reflective everywhere. The location of the first obstacle is $[1.3, 3.3] \times [0, 2.6]$ and the second one is $[5.1, 8.3] \times [0, 4.3]$. The terminal time is $t = 1.4$. The parameters are set as $\gamma = 1.2$, $q = 50$, $\tilde{T} = 20$, $\tilde{K} = 2410.2$.



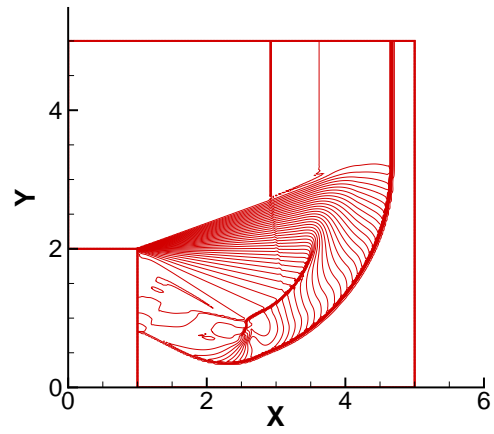
(a) Colored contour of density



(b) Contour line of density



(c) Colored contour of pressure



(d) Contour line of pressure

Figure 4.5: Detonation diffraction at a 90° corner.

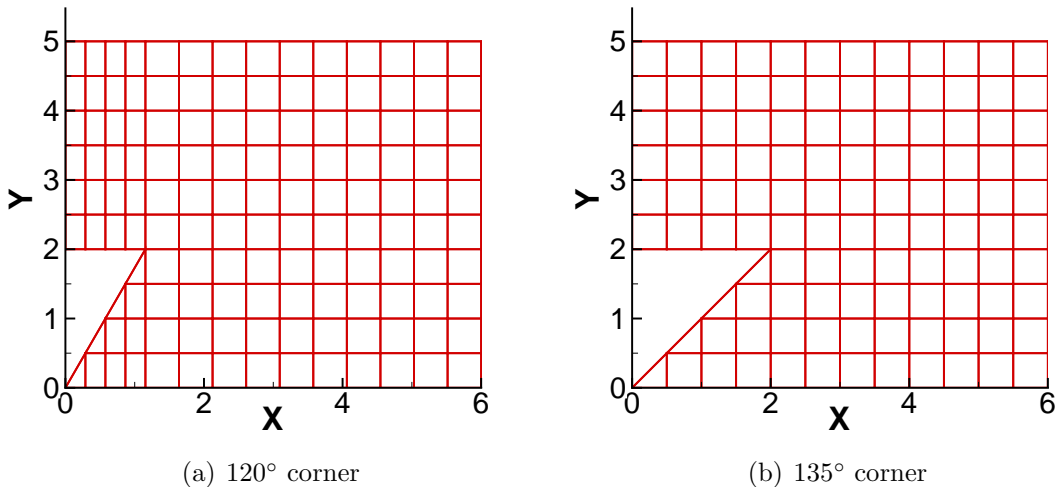
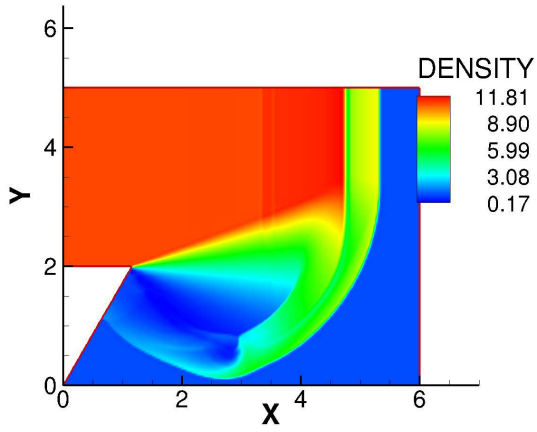


Figure 4.6: Illustrations of the meshes.

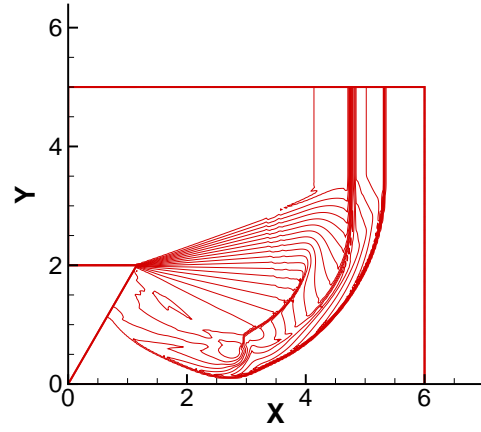
The mesh is non-uniformly rectangular. See Figure 4.9 for the result where the length of the smallest edge in the mesh is $\frac{0.85}{32}$.

5 Concluding remarks

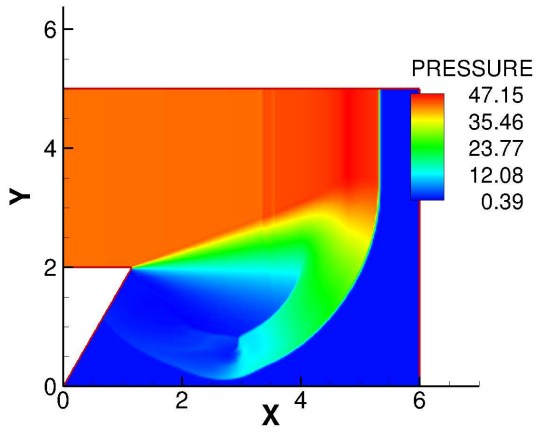
We have shown an extension of the positivity-preserving techniques in [22, 24, 23] to construct robust high order RKDG schemes for reactive Euler equations modeling gaseous detonations. Numerical tests suggest that the positivity-preserving limiter is sufficient to stabilize the high order DG method without the TVB limiter, and robust high order RKDG schemes can successfully simulate detonation diffraction cases in which the density or pressure of the numerical solution may become negative easily without the positivity-preserving limiter. In future work, we will use the RKDG schemes to carry out numerical simulation on gaseous detonation in more complex geometrical configurations in order to have more comprehensive insight of its propagation mechanism.



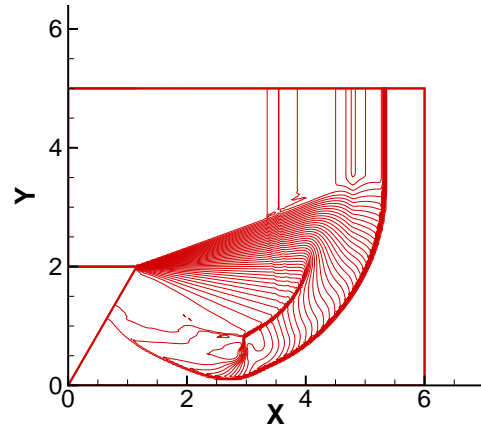
(a) Colored contour of density



(b) Contour line of density

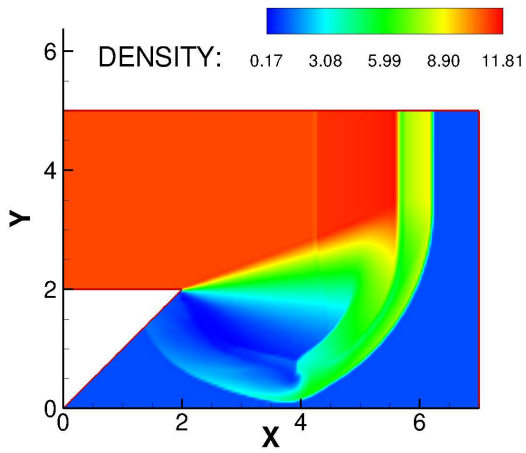


(c) Colored contour of pressure

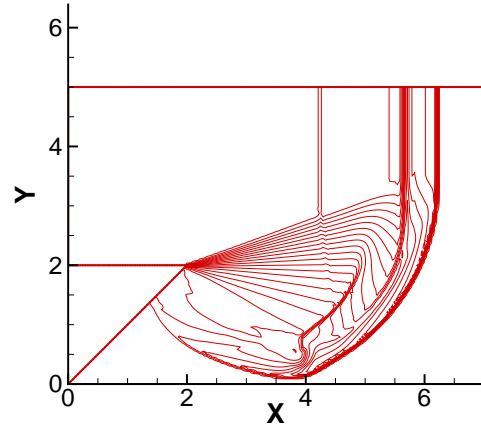


(d) Contour line of pressure

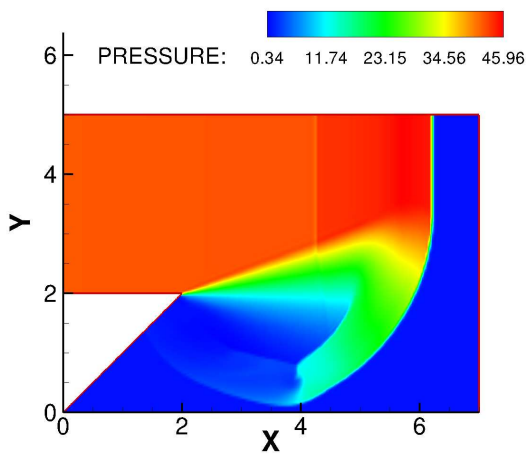
Figure 4.7: Detonation diffraction at a 120° corner.



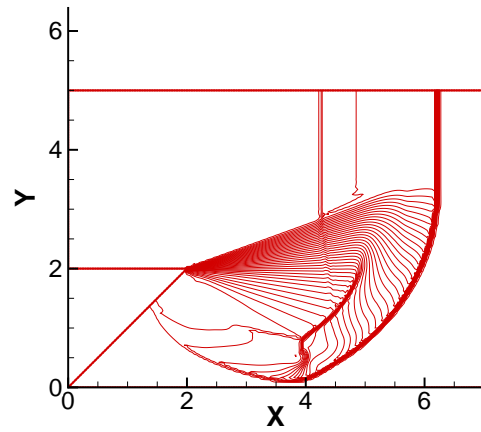
(a) Colored contour of density



(b) Contour line of density



(c) Colored contour of pressure



(d) Contour line of pressure

Figure 4.8: Detonation diffraction at a 135° corner.

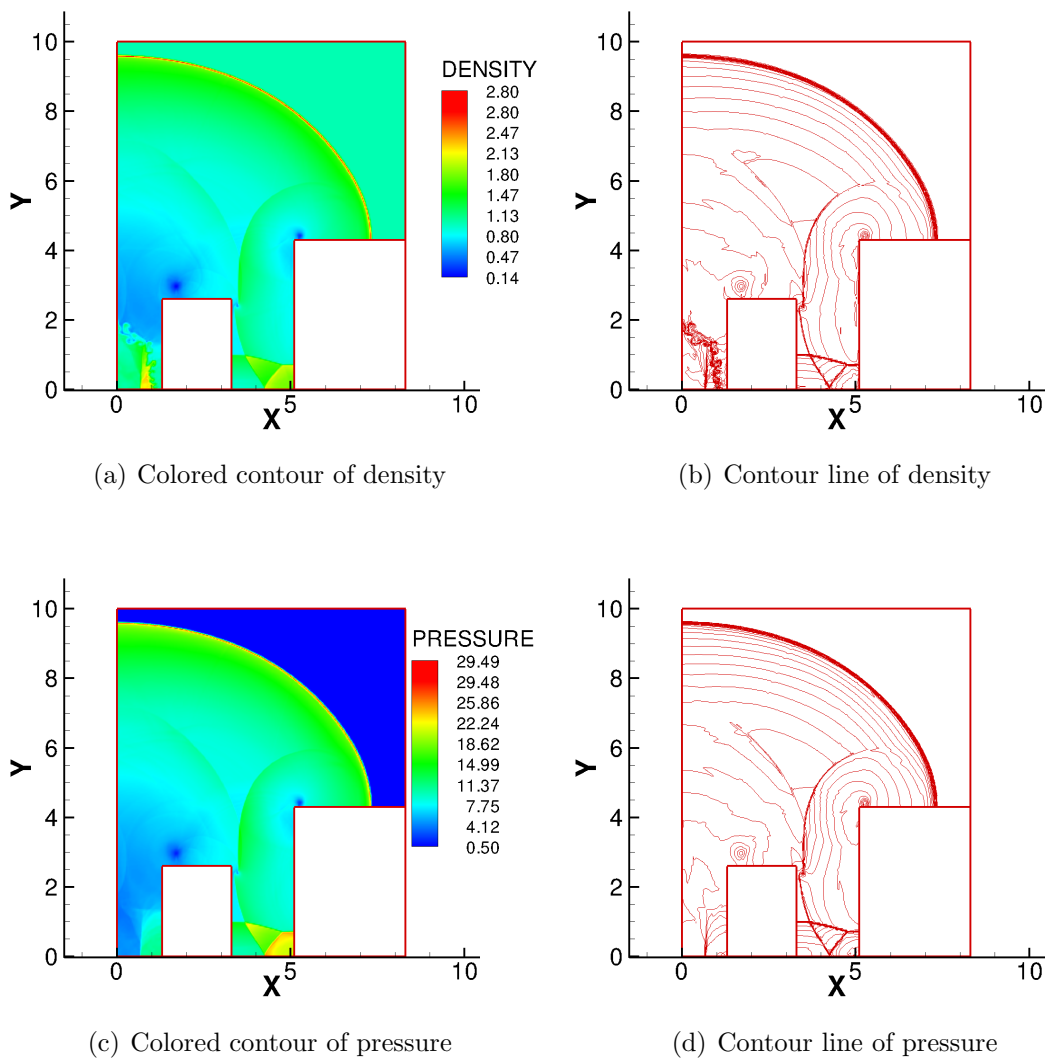


Figure 4.9: Multiple obstacles

References

- [1] B. Cockburn, S.-Y. Lin and C.-W. Shu, *TVB Runge-Kutta local projection discontinuous Galerkin finite element method for conservation laws III: one dimensional systems*, Journal of Computational Physics, 84 (1989), 90-113.
- [2] B. Cockburn and C.-W. Shu, *The Runge-Kutta discontinuous Galerkin method for conservation laws V: multidimensional systems*, Journal of Computational Physics, 141 (1998), 199-224.
- [3] J.F. Clarke, S. Karni, J.J. Quirk, P.L. Roe, L.G. Simmonds and E.F. Toro, *Numerical computation of two-dimensional unsteady detonation waves in high energy solids*, Journal of Computational Physics, 106 (1993), 215-233.
- [4] H.-S. Dou and B.C. Khoo, *Effect of initial disturbance on the detonation front structure of a narrow duct*, Shock Waves, 20 (2010), 163-173.
- [5] H.-S. Dou, H.M. Tsai, B.C. Khoo and J. Qiu, *Simulations of detonation wave propagation in rectangular ducts using a three-dimensional WENO scheme*, Combustion and Flame, 154 (2008), 644-659.
- [6] B. Einfeldt, C.D. Munz, P.L. Roe and B. Sjögreen, *On Godunov-type methods near low densities*, Journal of Computational Physics, 92 (1991), 273-295.
- [7] A. Harten, B. Engquist, S. Osher and S. Chakravarthy, *Uniformly high order essentially non-oscillatory schemes, III*, Journal of Computational Physics, 71 (1987), 231-303.
- [8] G.-S. Jiang and C.-W. Shu, *Efficient implementation of weighted ENO schemes*, Journal of Computational Physics, 126 (1996), 202-228.
- [9] R.J. LeVeque and H.C. Yee, *A study of numerical methods for hyperbolic conservation laws with stiff source terms*, Journal of Computational Physics, 86 (1990), 187-210.

- [10] T. Linde and P.L. Roe, *Robust Euler codes*, Thirteenth Computational Fluid Dynamics Conference, AIAA Paper-97-2098.
- [11] X.-D. Liu, S. Osher and T. Chan, *Weighted essentially non-oscillatory schemes*, Journal of Computational Physics, 115 (1994), 200-212.
- [12] T.-B. Ma, C. Wang and J.-G. Ning, *Multi-material Eulerian formulation and hydrocode for the simulation of explosions*, Computer Modeling in Engineering & Sciences, 33 (2008), 155-178.
- [13] J.-G. Ning and L.-W. Chen, *Fuzzy interface treatment in Eulerian Method*, Science in China Series G: Physics, Mechanics & Astronomy, 47 (2004), 550-568.
- [14] B. Perthame, *Second-order Boltzmann schemes for compressible Euler equations in one and two space dimensions*, SIAM Journal on Numerical Analysis, 29 (1992), 1-19.
- [15] B. Perthame and C.-W. Shu, *On positivity preserving finite volume schemes for Euler equations*, Numerische Mathematik, 73 (1996), 119-130.
- [16] Q. Qu, B.C. Khoo, H.-S. Dou and H.M. Tsai, *The evolution of a detonation wave in a variable cross-sectional chamber*, Shock Waves, 18 (2008), 213-233.
- [17] C.-W. Shu and S. Osher, *Efficient implementation of essentially non-oscillatory shock-capturing schemes*, Journal of Computational Physics, 77 (1988), 439-471.
- [18] C.-W. Shu, *Total-Variation-Diminishing time discretizations*, SIAM Journal on Scientific and Statistical Computing, 9 (1988), 1073-1084.
- [19] C. Wang, T.-B. Ma and J. Lu, *Influence of obstacle disturbance in a duct on explosion characteristics of coal gas*, Science China: Physics, Mechanics & Astronomy, 53 (2010), 269-278.
- [20] B.L. Wescott, D. Scott Stewart, and J.B. Bdzil, *On self-similarity of detonation diffraction*, Physics of Fluids, 16 (2004), 373-384.

- [21] X. Zhang and C.-W. Shu, *On maximum-principle-satisfying high order schemes for scalar conservation laws*, Journal of Computational Physics, 229 (2010), 3091-3120.
- [22] X. Zhang and C.-W. Shu, *On positivity preserving high order discontinuous Galerkin schemes for compressible Euler equations on rectangular meshes*, Journal of Computational Physics, 229 (2010), 8918-8934.
- [23] X. Zhang and C.-W. Shu, *Positivity-preserving high order discontinuous Galerkin schemes for compressible Euler equations with source terms*, Journal of Computational Physics, 230 (2011), 1238-1248.
- [24] X. Zhang, Y. Xia and C.-W. Shu, *Maximum-principle-satisfying and positivity-preserving high order discontinuous Galerkin schemes for conservation laws on triangular meshes*, Journal of Scientific Computing, to appear (doi:10.1007/s10915-011-9472-8).